Mapping the spatial variability of *Botrytis* bunch rot risk in vineyards using UAV multispectral imagery

Sergio Vélez [*], Mar Ariza-Sentís , João Valente

Information Technology Group, Wageningen University & Research, 6708 PB Wageningen, the Netherlands

A B S T R A C T

The fungus *Botrytis cinerea* causes severe diseases in many crops. In grapevines, it causes *Botrytis* bunch rot (BBR), one of the most reported diseases worldwide. It affects all herbaceous organs of the vine, especially the ripe berries, causing significant reductions in yield and wine quality. *Botrytis* detection models traditionally focus on temporal analysis at a specific spatial location, ignoring the study of the spatial variability of the crop. Unmanned aerial vehicles (UAVs) equipped with multispectral cameras can provide high-resolution images that can be valuable information to develop a tool for aerial pest detection. This paper proposes an algorithm to assess the risk of *Botrytis* development in a vineyard in Spain, using as input products generated by UAV imagery: DTM (Digital Terrain Model), NDVI (Normalised Difference Vegetation Index), CHM (Canopy Height Model) and LAI (Leaf Area Index). They represent the height and architecture of the canopy, the topography and the plant status. Healthy vines were significantly different from vines affected by *Botrytis* ($p < 0.05$) in each of these variables, supporting the consistency of using these inputs for the model. This methodology combines photogrammetric, spatial analysis techniques, and machine learning classification methods with deep vineyard-related agronomic knowledge to produce heatmaps with acceptable accuracy ($R^2 > 0.7$) that may support vineyard managers in understanding the spatial variability of the disease, allowing the spatial 2D visualisation of the risk of BBR disease development and, potentially, resulting in higher operational efficiency and reducing phytosanitary treatments, as well as economic costs. Furthermore, the present work takes advantage of imaging technologies that provide information about any location in the field, not only about specific points in the vineyard, suggesting that UAV imagery is appropriate to measure the likelihood of BBR development within the vineyard, highlighting the importance of efficient disease management based on spatial variability.

1. Introduction

The fungus *Botrytis cinerea* causes numerous types of diseases in many plants. Particularly, grey moulds are among the most important diseases of many crops and can be severe and economically damaging (Agrios, 2005). It causes *Botrytis* bunch rot in grapevines (BBR), a disease that affects all herbaceous organs of the vine, especially ripe berries, and causes significant reductions in yield and wine quality, having a major influence on the aromatic profiles of wines (Agrios, 2005; Elmer and Michailides, 2007; Lopez Pinar et al., 2017). It is the third most reported disease in European, North American and Australian vineyards, and the first cause of infection in irrigated vineyards in South America (Bois et al., 2017). The infection can progress on vines at any phenological stage, although from berry ripening onwards, the grapes may be more susceptible (Kretschmer et al., 2007), caused by various

factors, e.g. the presence of sugars, which diffuse through the berry skin and are available for fungal growth before penetration (Kosuge and Hewitt, 1964). The fungus also affects alternative hosts, including herbicide-treated or senescing weeds and other crops. It overwinters on several sources, such as fruit and prunings left on the ground or grape clusters and canes left on vines (Elmer and Michailides, 2007).

Typically, the protocol for managing the disease is based on a routine application of fungicides at specific phenological stages, resulting in unnecessary and redundant treatments as the actual risk of disease development is not considered. González-Domínguez et al. (2019) report that the number of sprays needed to control BBR in a vineyard can vary based on several factors, such as weather conditions, variety, microclimate, canopy structure or the presence of previous disorders. Apparently, this decision can be simplified by the use of models to predict the risk of developing the disease, which usually try to explain

---

the occurrence of BBR at a given time using physical variables, such as weather (Hill et al., 2019) or including specific parameters related to the phenology of the vineyard (González-Domínguez et al., 2015; Molitor et al., 2016; Fedele et al., 2020), however, in most cases, the results only represent a specific location where the measurements have been taken. In addition, they frequently consider pathogen-related variables; still, they do not consider host-related variables, such as the state of the plants, their agronomic characteristics or the growth of each plant. In other words, the spatial variability of the vineyard.

Consequently, it could be useful to develop models that complement them and allow the creation of maps, creating different zones in the plot according to their vulnerability, and helping the vineyard manager in the decision-making process. To this end, using remote sensing and multispectral imagery can be beneficial, improving site-specific management and allowing the creation of operational maps, such as prescription maps, to optimise field operations like phytosanitary treatments that can be loaded into variable-rate machines. This approach will result in a better crop assessment, a reduction of costs in crop management and higher environmental sustainability (Ammoniaci et al., 2021). Remote sensing includes many different technologies, including several platforms and sensors, which result in different resolutions and spectral data quality. Resolution is a critical factor for developing a disease diagnosis tool that assesses spatial variability since higher resolution allows for avoiding the effect of large pixels, such as including the information of several plants simultaneously, soil and shadows (Vélez et al., 2020). Moreover, enough spatial resolution will avoid capturing the entire canopy simultaneously, mixing healthy areas and those affected by disease or nutrient deficiency, leading to a systematic underestimation of the values extracted from the images compared with real observations (Marciniak et al., 2015). Therefore, photogrammetric techniques and multispectral cameras, combined with unmanned aerial vehicles (UAVs), can provide valuable information for multiple agricultural applications, such as evaluating water stress, monitoring the health status of the vegetation, and identifying spatial variability in the fields for variable rate pesticide application (Radoglou-Grammatikis et al., 2020). Moreover, it is possible to integrate UAV imagery in workflows aiming to improve the efficiency in the use of agricultural inputs based on the field spatial variability (Messina et al., 2021).

Many crop diseases can be successfully detected and mapped using aerial imagery (Zhang et al., 2021). However, each disease has its own development and particularities, conditioned by several factors that require different strategies for its control (Yang, 2020). To develop these strategies, knowledge and new approaches are needed to convert remote sensing data into useful prescription maps for farmers and vineyard managers. Most solutions based on aerial imagery largely rely on the exploitation of 2D products, without exploiting the possibilities of using the vast amount of information generated by the photogrammetric workflow. However, 3D products, such as classified point clouds, can improve the final product usefulness because of the addition of the third dimension of the crop (del-Campo-Sanchez et al., 2019). In this sense, Structure from Motion (SfM) is of special relevance within the photogrammetric workflow. SfM is a technique that can create high-quality, dense 3D point clouds of an object or a surface that combines advances in computer vision and traditional photogrammetry (Carrivick et al., 2016). It allows the creation of DSMs (Digital Surface Models), including DTMs (Digital Terrain Models), and enables the construction of CHMs (Canopy Height Models) to estimate plant height, achieving reasonable accuracy (Xie et al., 2021). The height of the canopy is a critical factor since canopy architecture affects plant health and the occurrence of diseases such as *Botrytis* (Kraus et al., 2018). Higher vineyards result in larger shades at canopy bases and changes in the canopy microclimate, affecting the cluster environment and significantly impacting the fruit exposure to radiation, leading to an increased *Botrytis* incidence (Smart et al., 2017).

Botrytis cinerea needs several conditions for its development. In this way, liquid water and high relative humidity promote disease development (Williamson et al., 1995; Cotoras et al., 2009). Consequently, it is important to consider variables that affect the relative humidity and the microclimate of the plant, such as the differences in topography. For example, the depressed areas will accumulate higher relative humidity in terrains with differences in altitude. Therefore, low spots where cold air ponds should be avoided because cold air is denser than warm air, so it flows downhill and accumulates in these spots, lowing the temperature and easing the condensation (Snyder and Abreu, 2005).

Another critical parameter is the canopy characteristics since they affect the microclimate of the bunches and their sun exposure. The canopy leaf area and its structure influence the radiation balance of the plant (Baeza et al., 2010), and are related to the risk of cryptogamic diseases (Hidalgo, 2006). The more humid the microclimate around the grape clusters, the higher the risk of grey mould (Bois et al., 2017), forcing practices such as leaf removal to reduce the incidence of *Botrytis* infections due to increased sun exposition (Creasy and Creasy, 2009).

Finally, another common approach to canopy assessment is using vegetation indices since they help to study the plant status. NDVI, or Normalised Difference Vegetation Index (Rouse et al., 1973), is one of the most used indices in viticulture (Giovos et al., 2021), and it has proven to be a valuable tool in viticulture for a wide range of applications (Urretavizcaya et al., 2014; Sun et al., 2017; Anastasiou et al., 2018; Vélez et al., 2020). It employs Red and Near-Infrared bands, and it is based on the fact that healthy plants show high near-infrared reflectance (NIR) and very low red reflectance (Lambers and Oliveira, 2019). NDVI has also been associated with plant vigour and other parameters measured in the field, such as leaf area (L. F. Johnson et al., 2001; Johnson et al., 2003; Towers et al., 2019; Matese and Di Gennaro, 2021) or the spatial variability of the vineyard (Baluja et al., 2012; Ledderhof et al., 2016; Pádua et al., 2019). Moreover, NDVI correlates with vine vigour, and the latter is linked to bunch compactness, favouring the development of BBR (Keller et al., 2001). It has been identified as a significant factor of prime importance concerning *Botrytis* development in vineyards (Pañitrur-De la Fuente et al., 2020).

Therefore, it is essential to include factors that estimate the vigour and status of the plant, the shading and microclimate of the cluster, and the water availability for the pathogen. In addition, other factors affect the BBR development in vineyards, e.g. monitoring the cluster can provide valuable information even if the disease has not yet developed. The compactness of the bunch is another critical aspect since it is considered one of the main factors affecting the development of *Botrytis cinerea* (Elmer and Michailides, 2007), and it is possible to automatically assess the degree of cluster compaction (Tello and Ibáñez, 2018). Still, using the images under real field conditions is challenging because the flight must take place at angles other than nadir, and clusters are usually underneath the leaves. Furthermore, leaf occlusion has been reported as a significant challenge in fruit detection, causing inaccuracies in fruit localisation (Gongal et al., 2015), forcing leaf removals to correctly identify and study the clusters (Font et al., 2015; Torres-Sánchez et al., 2021). Consequently, cluster assessment is time-consuming and costly, and only a fraction of the vineyard managers usually implement it. Thus, a risk assessment tool should be based on factors that can be estimated quickly in vineyards under standard management.

Based on a real case study in viticulture, UAV multispectral imagery is used in the present work as the input to develop a methodology for creating heatmaps of areas vulnerable to *Botrytis*. In order to generate *Botrytis* risk maps, the current approach considers DTM, NDVI, CHM and LAI (Leaf Area Index) estimated from multispectral images. The main highlights of this article are two: 1) provide the first methodology to assess the spatial variability of *Botrytis cinerea* development using UAV multispectral imagery in a vineyard, and 2) generate a novel approach using a new rationale, based on risk assessment, complementary to other models to optimise the *Botrytis* detection and consequently the phytosanitary treatment application.

2. Materials and methods

2.1. Vineyards

The experiment was carried out during the 2021 campaign, using a dataset from a 1.06 ha and 8.1 % slope commercial vineyard, *Vitis vinifera* cv. Loureiro, located in 'Tomiño, Pontevedra', Galicia, Spain (X: 516989.02, Y: 4644806.53; ETRS89 / UTM zone 29 N), property of 'Bodegas Terras Gauda, S.A.' (Fig. 1). The vineyard belongs to 'Rias Baixas AOP' (Appellation of Origin). The plants were grafted on 196.17 C rootstock, resistant to active limestone and suitable for soils with excessive humidity, trained in vertical shoot positioning (VSP), and planted in 1990 with a NE-SW orientation and a 2.5 × 3 m distance between plants and rows, respectively. The vineyard was managed according to the AOP protocol and legislation in force, and spontaneous vegetation species grew as cover crops.

The veraison phenological stage (onset of the ripening) was around 5 August 2021, showing phenology dynamics similar to previous years. Additionally, climate data was collected from the closest weather station ('Paramos. Val do Dubra'). The average temperature and relative humidity values from 1 April to 30 September were 17.5 ºC and 78.5 %, respectively. The cumulative rainfall for the period was 418 L/mm^2. The weather information can be found on the web service of the Meteorological Observation and Prediction Unit of Galicia (**https://www.meteogalicia.gal/web/inicio.action**, accessed on 2 May 2022).

2.2. Ground-truth data

The study was focused on three vineyard rows, including 153 grapevine plants (Table 1). Fig. 1 shows the ROI (Region of Interest) in red, which included a total investigated area of 1900 m^2. All plants within the ROI were considered, and each plant was accurately assessed on both sides to locate *Botrytis* disease in their clusters. *Botrytis* bunch rot was identified according to the literature: it produces grey mycelium and long, branched conidiophores with rounded apical cells bearing clusters of colourless or grey, one-celled, ovoid conidia (Agrios, 2005). The threshold for detecting *Botrytis* disease infection (Fig. 2) was established following the recommendations proposed by the European and Mediterranean Plant Protection Organization, EPPO (2002), marking the 'presence of *Botrytis* disease' as 'positive' from EPPO scale levels 2–5 and 'negative' for EPPO scale level 1, according to standard PP 1/17, *Botrytis cinerea* on grapevine (Anon, 2001). As a result, a total of 94 BBR-affected clusters were found across all plants within the ROI.

Table 1
Ground truth data. Affected clusters: number of affected grape clusters per plant. Number of plants: the number of plants found for that level of affected grape clusters.

| Affected clusters	Number of plants
0	91
1	42
2	13
3	3
4	3
5	1
Total number of plants	153

Each infected cluster was georeferenced using a Trimble R2 Integrated GNSS system with a TSC3 Controller (Trimble Inc., California, USA) capable of delivering centimetre positioning accuracy.

2.3. UAV imagery acquisition and processing

Before the UAV flight, seven ground control points (GCPs) were located in the vineyard and georeferenced using the Trimble R2 Integrated GNSS system to improve the geometric accuracy of the image mosaicking process.

The Unmanned Aerial System (UAS, Fig. 3) was composed of a DJI M210 multi-rotor platform UAV (DJI Sciences and Technologies Ltd., Shenzhen, Guangdong, China) and a Micasense RedEdge 3 multispectral camera (AgEagle Sensor Systems Inc., Wichita, Kansas, USA), equipped with a 4.8 mm × 3.6 mm sensor size, with a 3.75 μm pixel size, 1280 × 960 resolution for each one of the bands (1.2 MP x 5 imagers, Table 2) and a 4:3 aspect ratio. Based on the information provided by the manufacturer, the focal length is 5.5 mm, with a field of view of 47.2 degrees horizontal and 35.4 degrees vertical. The camera has an f/2.8 aperture and was factory calibrated. The exposure time was 1/523 s, capturing 1 picture per second, storing the files in 16-bit TIFF RAW format and embedding metadata tags for each file in standard EXIF format.

The flight took place on 16 September 2021, the same date as the grape harvest, at 30 m height and nadir angle. The sky during the flight was clear, with some isolated clouds (between 0 and 1 Okta cloud cover conditions). As a result, 650 were captured, generating 3250 files (one per imager). The shadows of the plants were used to extract the plant canopy information, following Vélez et al. (2021) method, scheduling the mission in the afternoon, between 16:00 and 16:30 (solar time), with
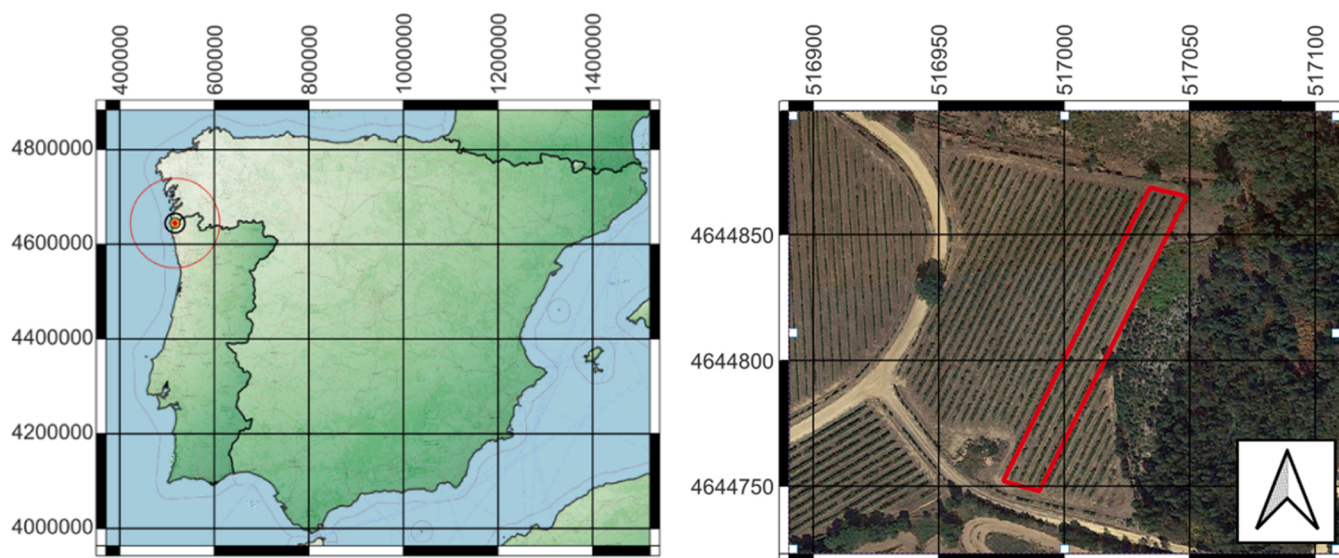
Fig. 1. Vineyard location ('Tomiño, Pontevedra', Galicia, Spain). Coordinates in ETRS89 / UTM zone 29 N.

Fig. 2. Example of clusters' positive' to 'Botrytis disease infection' detected in the vineyard (Vitis vinifera cv. Loureiro), located in 'Tomiño, Pontevedra', Galicia, Spain.

Fig. 3. Left: Unmanned Aerial System (UAS) composed of DJI M210 and Micasense RedEdge 3 multispectral camera. Right: Unmanned aerial vehicle (UAV) flight and detail of the vineyard and vegetation cover.

Table 2
Centre wavelengths and bandwidth.

Band	Centre	Bandwidth
Blue	475 nm	20 nm
Green	560 nm	20 nm
Red	668 nm	10 nm
Red edge	717 nm	10 nm
Near-infrared	840 nm	40 nm

a solar zenith angle (SZA) of 64°. For accurate reflectance data, pictures of the provided Micasense calibrated reflectance panel were captured from directly overhead it immediately before and after the flight. The UAV's horizontal speed was 2 m/s, and the flying height was 30 m above ground level (AGL) with an 80 % overlap. The Ground Sample Distance (GSD) estimated for the camera profile at the indicated flight height was 1.67 cm/px. To extend research on this topic and for reproducibility, the dataset used for this study was made available (Vélez et al., 2022).

The images were imported into Agisoft Metashape Professional software, v1.7.6 (Agisoft LLC, St. Petersburg, Russia), to process the images according to the software provider guidelines. Firstly, the locations of GCPs from the Trimble GNSS were located in the aligned images to optimise camera positions and orientation data and to improve orthophoto accuracy. Secondly, the pictures of the calibrated reflectance panel were identified to adjust the images according to the reflectance values provided by Micasense, and then the dense point cloud was created in Ultra High quality. Therefore, the dense point cloud was generated with the exact resolution as the raw images, without downscaling.

Initially, the DSM (Digital Surface Model) was generated using the complete dense point cloud. Moreover, an automatic classification of ground points and a mesh reconstruction were performed based on ground points only, generating the DTM (Digital Terrain Model). This process consisted of two steps: in the first one, the dense cloud was divided into cells of 10 m, detecting the lowest point within each cell and triangulating these points to create the terrain model. In the second step, the DTM is improved by adding new points if they lay within 1 m distance from the DTM and the angle between it and the line to connect this new point with a point from a ground class is less than 15°.

The computing platform was a high-performance computer with Linux 64-bit (Ubuntu 20.04.4 LTS). It was equipped with 64 Gb RAM, a Samsung SSD 860 EVO 1TB and an Intel(R) Core(TM) i9–10940X CPU processor with 14 cores (28 threads) and a base frequency of 3.30 GHz (4.80 GHz in Turbo Boost Max mode). Moreover, the computer includes two Nvidia Titan RTX, each with a Clock of 1770 MHz, 576 Tensor Cores, 4608 CUDA cores, and 24 GB GDDR6.

2.4. Botrytis risk algorithm

One of the paradigms of plant pathology is the disease triangle, composed of the pathogen, host and environment. Three components need to be aligned for a pathogen to develop into an epidemic successfully: the pathogen must be present, the host must be susceptible, and the environment must be conducive to the life cycle of the pathogen (Burchett and Burchett, 2017). Airborne fungal spores can often spread far away from the primary emission sources (Damialis et al., 2017). Specifically, airborne *Botrytis cinerea* spores can be virtually constant in the atmosphere (Rodríguez-Rajo et al., 2010) and overwinter on several sources within the vineyard. Therefore, a starting assumption of the algorithm is that the pathogen *Botrytis cinerea* is endogenously present in the vineyard as part of the microbiome environment (Keller et al., 2003;
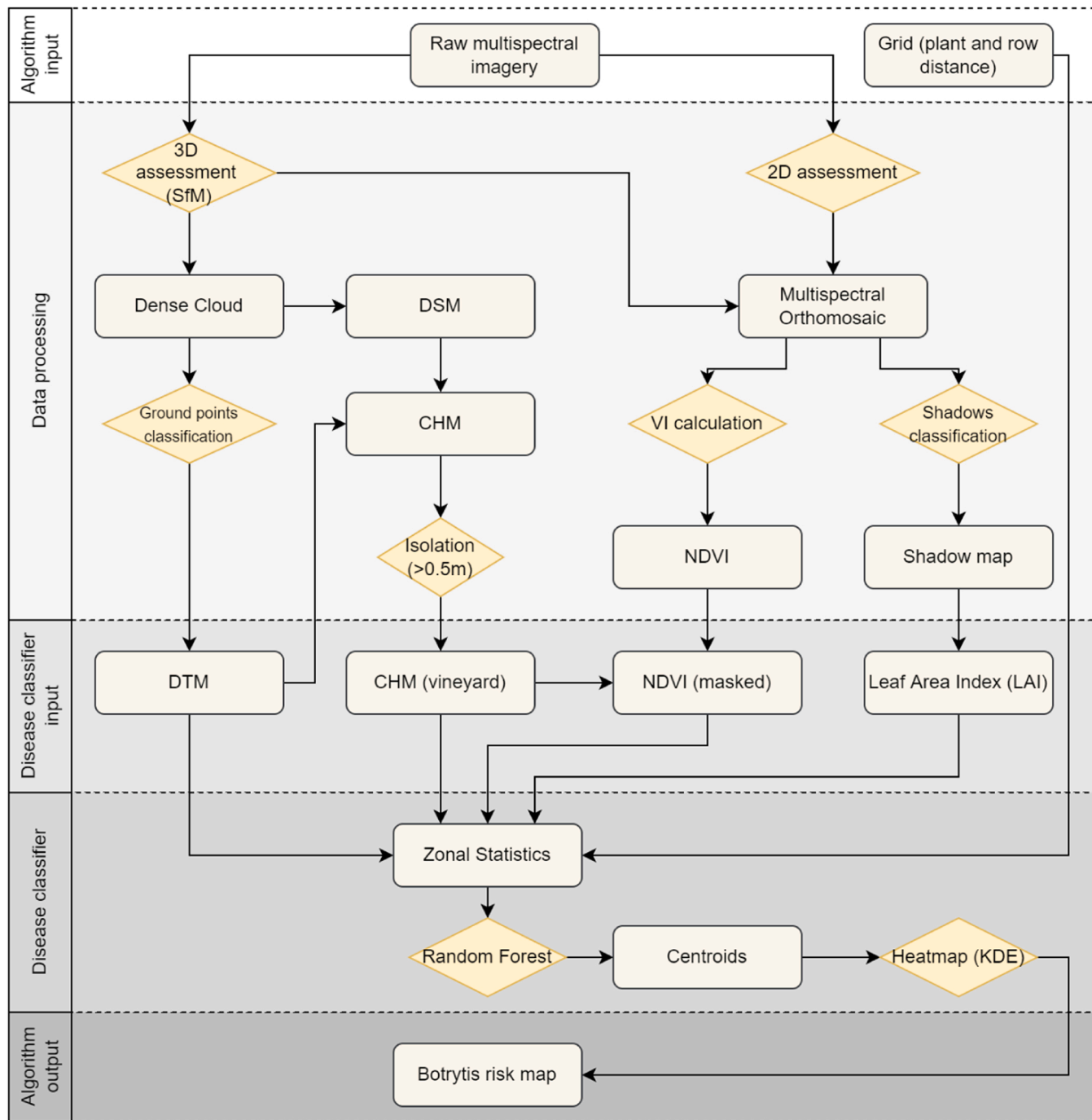

Fig. 4. – Workflow of the proposed methodology to obtain the Botrytis risk map. The initial inputs are the raw multispectral images and the grid defined by the distance between plants and rows. The inputs for the disease classifier are the DTM (Digital Terrain Model), CHM (Canopy Height Model), NDVI (Normalized Difference Vegetation Index) and LAI (Leaf Area Index). Finally, the Botrytis risk map is the predicted heatmap computed using Random Forest and kernel density estimation.

Elmer and Michailides, 2007), meaning that the disease will only develop if certain optimal conditions are met in the host and the environment.

Since leaf occlusion is a significant issue and grape clusters are usually underneath the leaves, an algorithm adapted to the limitations of nadir UAV multispectral imagery was developed (Fig. 4), processing the available spectral data to generate valuable information to assess some of these relevant factors for fungal development. Consequently, the conditions necessary for the development of the disease were divided into two main blocks: i) factors dependent on the host, such as canopy architecture, vine vigour and status, and ii) factors reliant on the physical environment, such as topography. Since UAV data is also valuable for topographic analysis based on photogrammetry (Avtar and Watanabe, 2020), DTM was selected to consider the effect of altitude, depressions or other changes in the topography that could affect the microclimate of the plant. Those related to plant development include LAI, CHM, and NDVI. The leaf area index (LAI) was estimated using shadows, following the method described by Vélez et al. (2021), without calibration for this specific vineyard. Therefore, the employed LAI was consequently a 'relative LAI' instead of actual LAI values. However, the absolute LAI values are not required, and the 'relative LAI' values for that orthomosaic are sufficient, as the final result is a probability map specific to this vineyard.

To estimate plant height, CHM was calculated as the difference between the DSM and the DTM (Eq. 1):

$$CHM = DSM - DTM \tag{1}$$

The NDVIwas firstly calculated using Red and NIR bands (Eq. 2), according to the following expression:

$$NDVI = \frac{(NIR - Red)}{(NIR + Red)} \tag{2}$$

However, NDVI includes any kind of vegetation, such as grapevines or weeds, without distinction (Avtar and Watanabe, 2020), and since the vineyard of the study had vegetation cover, NDVI was masked using CHM > 0.5 m to isolate the grapevine canopy. This step is unnecessary in a vineyard with bare soil because the grapevine pixels can be segmented using just NDVI values (Campos et al., 2021) and applying a certain threshold. After all, vegetation is distinguishable from other objects such as soil, rocks or dead wood.

In the algorithm workflow, as an initial step, the raw images are employed to build the point cloud and the orthomosaic, as well as the NDVI, LAI, DTM, and CHM, as described in Fig. 4. Once all these layers of information are available, a grid, based on the spacing between plants and rows (2.5 m x 3 m), is used to extract the information corresponding to each plant and develop a plant-based analysis. Thus, each tile of the grid contains one plant. In the next step, the Random Forest (RF) algorithm is used as a classification method to predict whether or not *Botrytis* will be developed in that plant. It is a supervised machine-learning method based on decision trees for classification and prediction and has already proven its usefulness in agriculture (Loggenberg et al., 2018; Siebring et al., 2019; Geetha et al., 2020; Zhang et al., 2021). The algorithm fits many classification trees into a dataset and then combines the predictions from all the trees (Kuhn, 2008). The dataset extracted from the zonal statistics step is used to train the RF algorithm. Each dataset row represents a plant, and the columns contain each variable metric (DTM, CHM, LAI, and NDVI). In addition, there is a column representing the plant's health status, which allows two labels: 'BOT' (plants affected by *Botrytis*) and 'noBOT' (healthy plants). The 'status' column is the one to be predicted by the algorithm while using the validation dataset.

Subsequently, the centroids of the tiles are computed to transform them into points, therefore, matching the theoretical location of the trunk of the plant. Finally, a heatmap is computed using kernel density estimation (KDE), producing a *Botrytis* risk map. Since the study is based on a physical phenomenon (the spatial distribution of a disease), the kernel density estimation method (Eq. 3) was chosen. For a given X_1 , ...X_n multivariate data set whose underlying density is to be estimated:

$$f(x) = \frac{1}{nh^d} \sum_{i=1}^{n} K\left\{\frac{1}{h}(x - X_i)\right\} \tag{3}$$

where $f(x)$ is the estimated density value at location x, n is the number of points, h is the kernel bandwidth, K is the kernel function, d is the number of dimensions and X_i is the location of point i. Therefore, $(x - X_i)$ is the Euclidian distance between each point i and the location of the density estimator (Silverman, 2018).

KDE can consider the spatial interdependency of data and calculates the density of points within a neighbourhood by adding the values of all kernel surfaces, depending on the bandwidth. In such a way, density is computed as a function of the frequency of points at a location, with a higher number of clustered points resulting in higher values. Heatmaps provide an easy way to identify hot spots and clustering of points.

Biweight was selected as kernel function $K(u)$, also known as Quartic (Eq. 4) since it is usually the default kernel in GIS software and it tends to produce smoother density maps (Diggle, 2013):

$$K(u) = \begin{cases} \frac{15}{16}(1 - u^2)^2 & , for |u| < 1 \\ 0, & otherwise \end{cases} \tag{4}$$

In order to define bandwidth h, Likelihood Cross Validation Bandwidth Selection for the kernel density algorithm was employed. It generates more appropriate values than other methods when the pattern predominantly comprises dense clusters instead of single clusters within random noise (Baddeley et al., 2016), as in the *Botrytis* case, where infections are spread from the source of inoculum. Moreover, it generally performs better than other algorithms if sample sizes are small (Horne and Garton, 2006). The algorithm proposed a bandwidth of $h = 19.68$.

Botrytis cinerea spores can spread from the emission sources, and the infection is more likely to develop in highly localised zones of disease pressure that can lead to the collapse of host resistance (Elad et al., 2007; Elmer and Michailides, 2007). Therefore, areas with dense point clusters will have higher chances of developing the disease. Heatmaps are a useful interpolation technique to assess the density of features in a specific area, showing the intensity of a particular event. This method calculates the density of points within a neighbourhood by adding the values of all kernel surfaces where they overlap, adjusting a smoothly curved area over each feature. If there are no close points to a particular cell (NoData), value 0 is assigned, meaning that the probability is 0 %. Finally, the heatmap is divided using the max value to compute final values ranging from 0 to 1. Thus, 0 % probability to 100% probability of disease development.

All layers are masked using the same ROI, according to the vineyard limits.

2.5. Validation

The 153 grapevine plants assessed were used as a ground-truth dataset, given that BBR was identified in each cluster. In order to validate the *Botrytis* risk map, a heatmap using ground-truth data was created employing kernel density estimation utilising the same parameters (same points and same bandwidth).

Initially, an exploratory data analysis using the Wilcoxon test on each variable was developed to detect significant differences ($p < 0.05$) between groups, healthy vines and vines affected by *Botrytis,* in each one of the selected factors.

Next, aiming to compare the estimated heatmap and the heatmap computed using the ground-truth data, each plant was tested for the likelihood of being affected by *Botrytis*. To this end, a calibration (cross-validated, 50 % split) and validation procedure was used to assess and

compare the ability of the model to predict *Botrytis*. The coefficient of determination (R^2) was used to indicate how well the model explained the observed results, validating the model's performance and the accuracy of the generated *Botrytis* risk map. This process was performed firstly using the location of the plants. Secondly, the results were validated in the ground points where *Botrytis* was detected because BBR can affect several clusters in each plant. Finally, since field measurements are punctual, 100 random points were generated within the ROI.

All image, statistical, and data analyses were carried out using QGIS (version 3.22. X, QGIS developer team 2022), and R software (version 4.2. X, R Foundation for Statistical Computing, R Core Team 2019, Vienna, Austria), including packages *spatstat*, *randomForest*, *raster*, *rgdal*, *sf*, *rgeos*, *caret* and *caTools*, obtained from the Comprehensive R Archive Network (CRAN).

3. Results

3.1. Exploratory analysis

First, the grid based on the spacing between plants and rows was employed to extract the information corresponding to each plant. In this way, NDVI, LAI, DTM, and CHM values were calculated on a plant-based approach. Table 3 shows an example of values used for statistical analysis.

An exploratory data analysis using the Wilcoxon test on each variable shows that there were significant differences ($p < 0.05$) between healthy vines ('noBOT') and vines affected by *Botrytis* ('BOT') in each one of the selected variables, confirming the initial assumption of integrating these variables in the model (Fig. 5). In this way, significant differences were found in the NDVI, with a mean value of 0.80 for plants affected by *Botrytis* and 0.78 for healthy plants. For the CHM, the mean values were 1.49 m for plants affected by *Botrytis* and 1.40 m for healthy plants. The DTM was generated with high accuracy ($R^2 > 0.99$, RMSE < 0.05), and the mean values were 72.32 m and 73.87 m for plants affected by *Botrytis* and healthy plants, respectively. The minimum altitude was 67.14 m, and the maximum was 75.76 m. And finally, the LAI values of plants affected by *Botrytis* were 0.51 and 0.38 for healthy plants.

3.2. Random forest classification

Once the consistency of using the cited variables is confirmed, the Random Forest algorithm is used as a classification method to predict whether or not *Botrytis* will be developed in that plant. To this end, RF was configured considering all variables (NDVI, CHM, DTM and LAI), the number of trees was set to 500, with a split ratio of 0.75, and all other parameters have been selected to default settings.

Fig. 6 shows the confusion matrix, categorising the predicted values (Y-axis) against the true values (X-axis). It is generated using Random Forest values based on the Out of bag (OOB) score, where 58 plants were assessed in total (0.75 split ratio). The results show a classification error of 0.19 when Random Forest predicts the presence of disease ('BOT') and 0.4 when Random Forest predicts there is no disease ('noBOT') with an OOB estimate of the error rate of 29.31 %.

The variable importance test shows how important each variable is in classifying the data. In this work, the most important factor is LAI (Fig. 7), followed by CHM and DTM. The least important factor was NDVI.

3.3. Heatmap generation – Botrytis risk map

Fig. 8 presents the results of the global workflow, including the generated products for the *Botrytis* risk algorithm. It shows the raw multispectral images and how they are employed according to the 2D and 3D assessments. First, the NDVI and the shadows used for computing the LAI were derived from the orthophoto; meanwhile, the DTM and CHM were produced using the dense point cloud. Then, the predicted heatmap was computed using Random Forest and kernel density estimation, and it was compared with the heatmap calculated using ground-truth data.

Fig. 9 presents the heatmaps (*Botrytis* risk maps) generated using kernel density estimation. The left map was built using the ground-truth data, and the right map was made using the Random Forest classification model results. The scale bar shows the relationship between the colour of each pixel displayed on the map and the probability values, where blue represents 0 % probability, and red indicates 100 % probability of *Botrytis* development.

Furthermore, the estimated probabilities of *Botrytis* development were compared with the observed values to assess the accuracy of the *Botrytis* risk algorithm. Fig. 10a shows the correlation using the locations of the plants within the ROI (according to the plant and row distance), resulting in an $R^2 = 0.71$. Fig. 10b illustrates a correlation of $R^2 = 0.68$, using only the ground points where *Botrytis* was detected. Finally, Fig. 10c shows the correlation using 100 random points generated within the ROI, giving an $R^2 = 0.72$.
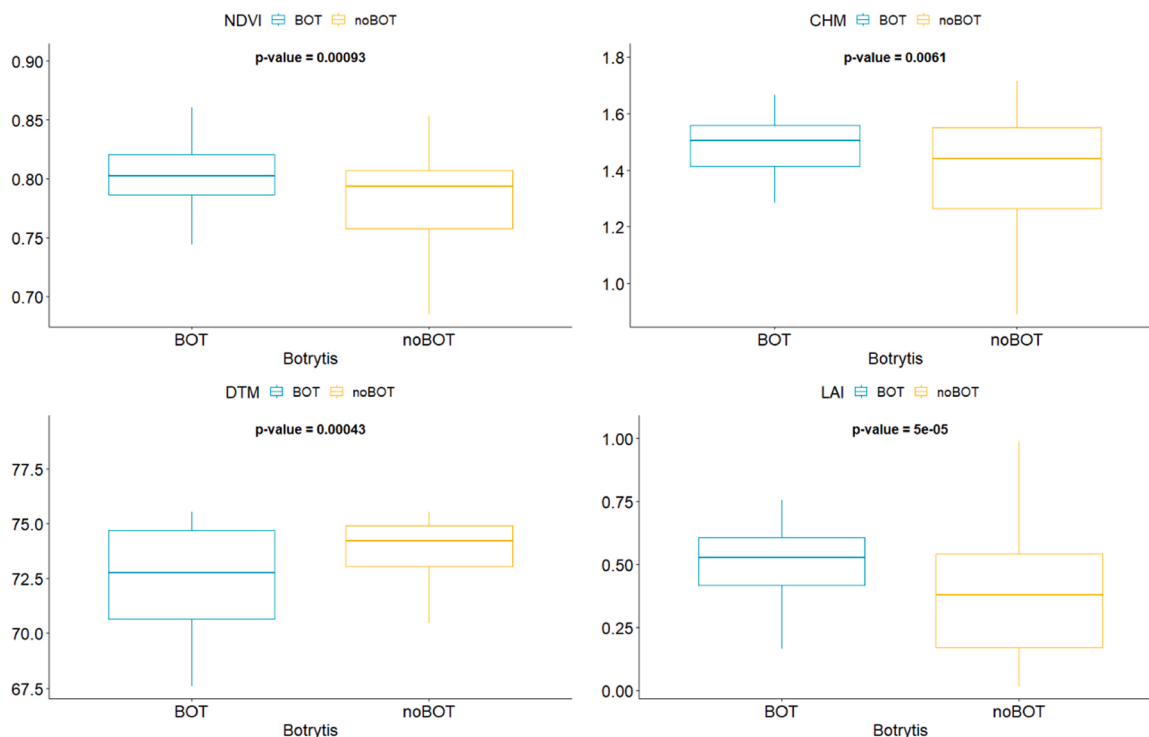
4. Discussion

4.1. Exploratory analysis

The exploratory study confirms that the four variables included in the algorithm were suitable for the model. The mean values for some variables were very similar, i.e. NDVI, with a difference of only 0.02 between the two groups. However, they all showed clear significant differences (p-value < 0.05). Other variables, such as LAI, showed a remarkable difference (0.51 vs 0.38), implying that plants affected by BBR had 25 % more LAI than those without it.

Regarding the vegetation indices, higher NDVI values are related to higher BBR incidence, confirming at harvest the results that Pañitrur-De la Fuente et al. (2020) found at veraison. It is well known that NDVI provides insights into vine vigour (Fuentes et al., 2014; Gatti et al., 2017; Campos et al., 2019, 2021; Pádua et al., 2019), which interacts with climate and microclimate, and it is positively correlated with BBR incidence at harvest (Valdés-Gómez et al., 2008) with high vigour vines showing more incidence of BBR and low vigour vines showing the lowest incidence (Ferrer et al., 2020). In addition, less vigorous and weaker grapevines tend to have less compact clusters and grapes with more tannins in the skin (Keller, 2015), which is closely related to the results of Pañitrur-De la Fuente et al. (2020), who found that reduced NDVI led to a significant rise in skin tannin content in herbaceous grapes at veraison, enhancing the biochemical defence mechanisms of the fruit due to the higher tannin composition of the berry skin. This finding is consistent with previous scientific literature because the total tannin content of grape skins affects fungal development and berry infection (Deytieux-Belleau et al., 2009).

As for the contribution of the height of the canopy to the disease development, the plants affected by BBR had higher CHM values than the healthy plants (1.49 m vs 1.40 m), supporting that high height values modify the exposure to radiation, affecting the microclimate of the cluster and contributing to the emergence of the disease.

Concerning the topography of the terrain, the results align with the

Table 3
Example with values used for statistical analysis. NDVI (Normalized Difference Vegetation Index, dimensionless), CHM (Canopy Height Model, m: meters), DTM (Digital Terrain Model, meters), LAI (Leaf Area Index, dimensionless). Label: 'BOT' (plants with BBR) and 'noBOT' (plants without BBR).

Plant id	NDVI	CHM	DTM	LAI	Label
62	0.777047	1.537478	75.28817	0.465191	noBOT
63	0.806472	1.438717	75.29755	0.478284	BOT
67	0.722251	1.255826	74.98823	0.094943	noBOT

Fig. 5. Boxplots. Top-left: NDVI (Normalized Difference Vegetation Index, dimensionless), top-right: CHM (Canopy Height Model, m: meters), bottom-left: DTM (Digital Terrain Model, meters), bottom-right: LAI (Leaf Area Index, dimensionless). Groups: 'BOT' (plants with BBR) and 'noBOT' (plants without BBR). Significance level: p-value< 0.05 (Wilcoxon test).
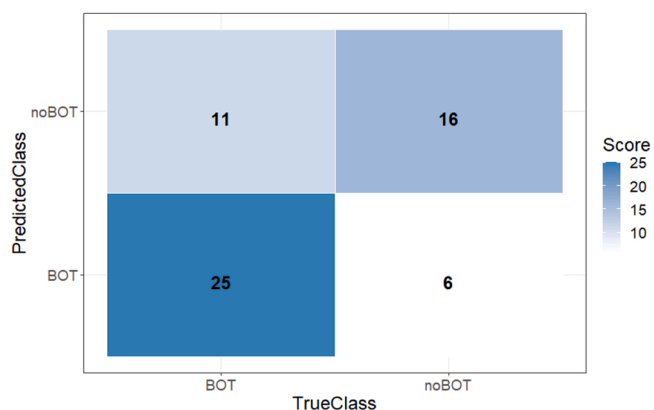
Fig. 6. Confusion matrix generated using Random Forest values based on OOB data. 58 plants were assessed in total. Groups: 'BOT' (plants with BBR) and 'noBOT' (plants without BBR).

initial hypothesis that it affects the development of the disease. Areas with lower altitudes are related to a higher development of *Botrytis cinerea*, showing an average difference of 1.5 m altitude between infected and non-infected plants. One hypothesis could be that, in the same area, bottom areas are more likely to accumulate cold air and high relative humidity (White, 2015), which promotes the appearance of liquid water and favourable conditions for the development of the fungus. In this vineyard, the minimum altitude is 67.14 m, and the maximum is 75.76 m; however, this factor will probably not be relevant in a vineyard on flat terrain or with slight slopes.

And finally, with regard to canopy architecture, BBR-affected plants had, on average, 25 % higher LAI values than healthy plants. This result is explained mainly by the architecture of the canopy, which defines the microclimate of the plant and the cluster, affecting key factors such as sun exposure and relative humidity around the cluster (Hidalgo, 2006;

Baeza et al., 2010; Bois et al., 2017). Therefore, this variable is critical and very interesting to be monitored since the vineyard manager can more easily influence the LAI than the other variables studied, i.e. by removing leaves (Creasy and Creasy, 2009). In this sense, *Botrytis cinerea* infection progression rate is slower when plants are subjected to leaf removal management (Würz et al., 2021), confirming that the leaf area is closely related to the development of the disease.

4.2. Botrytis risk algorithm

So far, the results highlighted in this article are consistent with other literature results (White, 2015; Pañitrur-De la Fuente et al., 2020; Würz et al., 2020), showing that vine vigour, topography, canopy architecture and plant status assessed using vegetation indices are key features to better understanding the probability of being affected by BBR.

Based on the computed values of DTM, CHM, NDVI, and LAI, Random Forest was able to predict whether a plant would develop BBR or not with an estimated error rate of 29.31 %. According to the variable importance test, the Random Forest classification ranked the most relevant variables as LAI, CHM, DTM and NDVI. Mean Decrease Accuracy indicates how much the accuracy drops down when a variable is left out of the model. The more the accuracy is impacted, the more critical the variable is for modelling. On the other hand, the Mean Decrease Gini is a variable-importance measure based on the Gini impurity index that is used to calculate tree splits. It is a measurement of the contribution made by each variable to the homogeneity of the resulting Random Forest's nodes and leaves, and, once more, the greater the score, the more significant the variable is in the model.

The results are consistent with what has been discussed above, as leaf area is closely related to the development of BBR and other cryptogamic diseases, affecting the microclimate around grape clusters (Hidalgo, 2006; Creasy and Creasy, 2009; Bois et al., 2017; Würz et al., 2020). In contrast, NDVI was the least related variable, which could be caused by the connection of NDVI with other factors than vigour, such as other diseases (Daglio et al., 2022), water status (Cancela et al., 2017; Ferrer
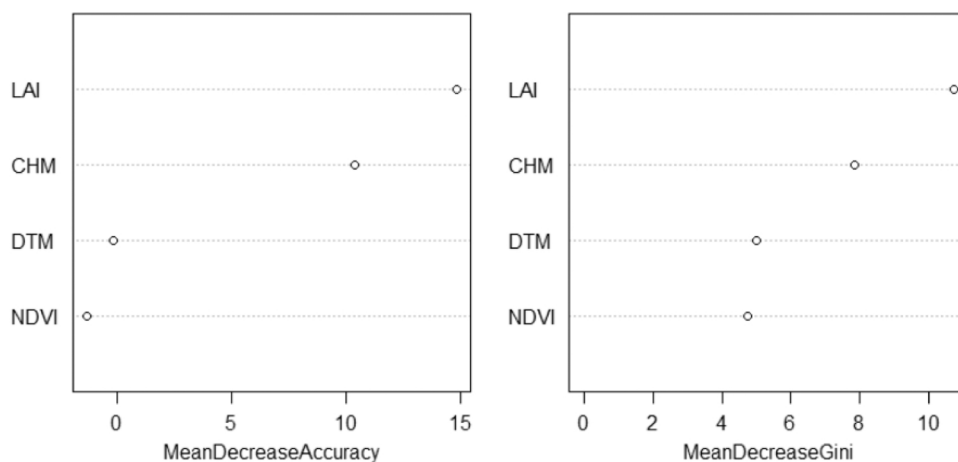
Fig. 7. Variable importance test generated from Random Forest, showing mean decrease accuracy and mean decrease Gini. NDVI (Normalized Difference Vegetation Index, dimensionless), CHM (Canopy Height Model, m: meters), DTM (Digital Terrain Model, meters), LAI (Leaf Area Index, dimensionless).
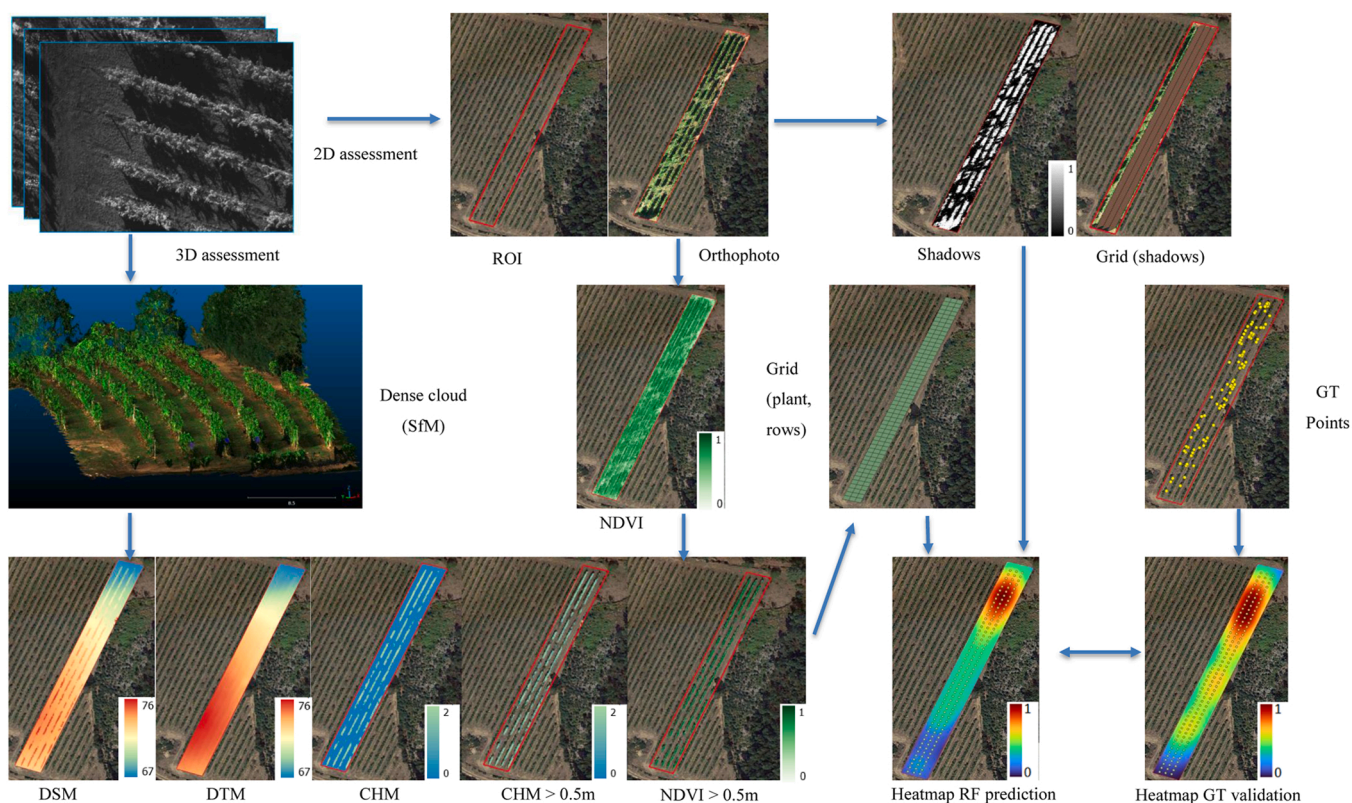

Fig. 8. Botrytis risk algorithm workflow, including generated products. The raw multispectral images were assessed using a 2D and 3D approach. The NDVI and the shadows for computing the LAI were derived from the orthophoto. Next, the DTM and CHM were calculated using the dense point cloud. Finally, the predicted heatmap was computed using Random Forest (RF) and kernel density estimation, and it was compared with the heatmap computed using GT (ground-truth) data. NDVI (Normalized Difference Vegetation Index, dimensionless), CHM (Canopy Height Model, m: meters), DTM (Digital Terrain Model, meters), LAI (Leaf Area Index, dimensionless).

et al., 2020) or the difficulty for NDVI to assess crop vigour when the ratio soil/canopy in the images is relevant (Matese and Di Gennaro, 2021). Nevertheless, NDVI was used in the present work because it is one of the most widely used indexes (Giovos et al., 2021) and, as mentioned earlier, its relation to *Botrytis cinerea* development (Pañitrur-De la Fuente et al., 2020). However, future algorithm versions could incorporate other vegetation indices or spectral information. Furthermore, Random Forest has been employed in this work, but future versions could modify this classifier using different machine learning algorithms.

At first glance, the *Botrytis* risk map resulting from the proposed algorithm was quite similar to the heatmap obtained from the ground-truth data (Fig. 9), with a red hotspot in the north part of the vineyard and a blue depression in the south. In addition, it shows clear zones that highlight *Botrytis* risk areas which are probably related to variations in the input variables employed for the model. In other words, in terms of risk, the top part of the vineyard is more vulnerable to BBR development, with two zones in the vineyard: the northern and southern, with the highest and the lowest probability scores, respectively. These two regions were also visible on the LAI and DTM maps, showing clear
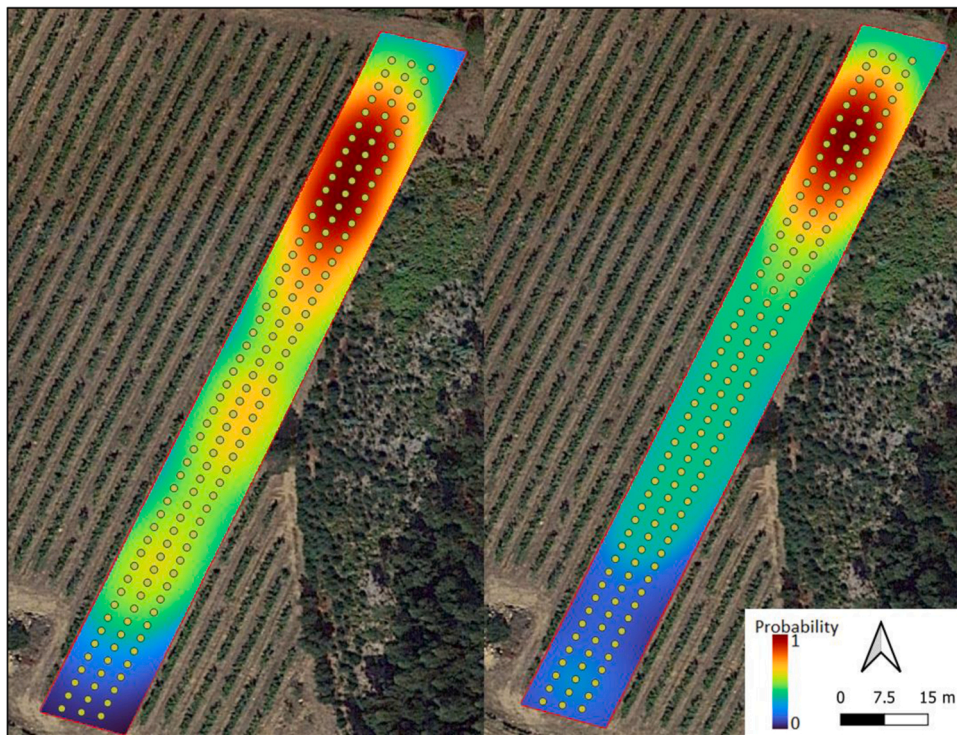
Fig. 9. Left: Heatmap generated using ground-truth data. Right: Heatmap generated using Random Forest prediction. The points are the positions of the plants, according to the plant and row distance.
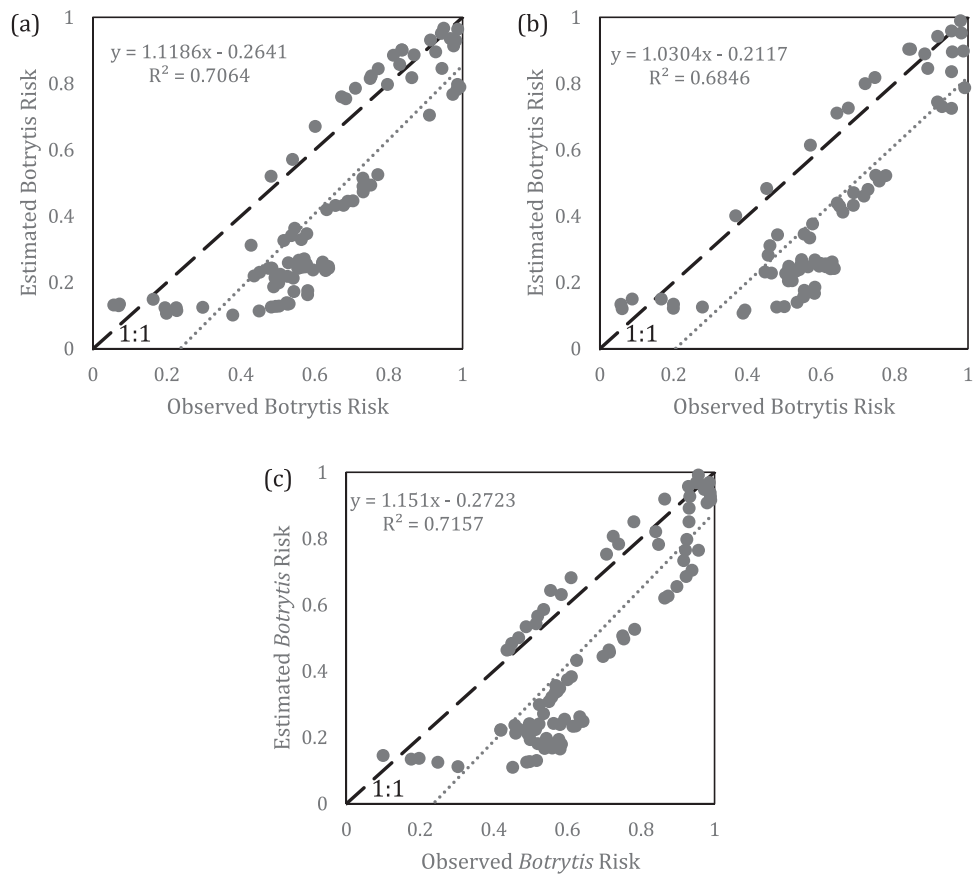

Fig. 10. Botrytis risk estimated vs predicted correlations according to heatmaps. Sample points: (a) Plants (b) Botrytis ground-truth points (c) Random Points within the ROI. Significance level: p-value< 0.05.

spatial patterns, with different sections consistent with the observations in the field (Fig. 8).

Both maps show high heterogeneity in the *Botrytis* risk assessment regarding spatial variability. This heterogeneity could be explained due to topography and vegetative development differences. Low LAI values and the absence of enough relative humidity to reach the dew point could be limiting factors related to the disease development that may explain the observed results. Furthermore, the vineyard experiences a slight depression in the northern part of the field, as can be visually appreciated in the DTM model, also overlapping with the LAI map, suggesting that these two variables are correlated. Not surprisingly, topography is essential for plant development since it affects critical factors such as water availability and soil variations related to the transport of soil materials to lower elevations (White, 2015).

The main advantage of plotting the information as heatmaps is getting a more precise spatial interpretation of the variation of *Botrytis* risk throughout the vineyard. Moreover, it also eases the visual comparison with the ground-truth data, giving an idea of the ability of the model to assess risk areas and produce helpful outputs for the vineyard manager. Additionally, a statistical analysis (Fig. 10) shows that the values are very similar for all sampling types (plants, ground data or random points). The coefficient of determination is very similar for each approach, ranging from 0.68 to 0.71, so it can be considered that the spatial consistency is good, especially bearing in mind that only UAV imagery was used. However, the proposed model underestimates the risk of *Botrytis* for all probability values. The explanation may lie in a number of factors, and it is hard to explain whether it is due to the variables used, the machine learning algorithm or the nature of the particular data of this vineyard. Still, the present article aims to propose a new and useful methodology to assess *Botrytis* risk in the vineyard, with agronomical significance: not to fit the data perfectly but to understand the relationship between the employed variables and the proposed methodology.

As previously stated, it is clearly recognised that there are more factors influencing the *Botrytis* development, especially weather-dependent variables such as rainfall or fogs combined with low temperatures leading to high relative humidity that contribute to the presence of free water on the surfaces, promoting the appearance of the disease (Williamson et al., 1995; Cotoras et al., 2009), as well as its aggressiveness, as they facilitate the formation of secondary infections via asexual conidia from sporulating host tissues. However, it is hard to estimate this information using UAV nadir images, requiring other information sources, computing techniques or sensors. Therefore, one of the limitations of the study is that the workflow does not include weather information, which indeed impacts the development of fungal diseases in vineyards. Another limitation would be that since this study considers a spatial approach, the quality and accuracy of the result will depend on the type, quality and resolution of the sensor and flight height. Finally, another limitation of the method is that all the factors considered in the workflow, except elevation, change throughout the year with the phenological cycle of the vineyard. Therefore, it is important to bear in mind the date of the mission, as the drone images are taken in missions programmed on specific dates and therefore do not perform continuous measurements like other kinds of sensors that can be installed in the field, such as weather or soil moisture sensors.

Nevertheless, the interest and novelty of the present work are based on the use of a single source of information (UAV nadir images) which, through different data processing methods, allows the creation of a *Botrytis* risk map to assess the spatial variability of the disease and can be very useful for the vineyard manager. So far, other *Botrytis cinerea* models published in the literature rely on individual instruments (Rodríguez-Rajo et al., 2010; González-Domínguez et al., 2015; Molitor et al., 2016; Reich et al., 2017; Hill et al., 2019; Fedele et al., 2020), such as relative humidity, soil moisture or temperature sensors, in very few locations, measuring information at that exact place for a certain period. Indeed, used wisely, these models can lead to a phytosanitary reduction related to fewer treatments due to the estimation of the optimal moment to carry them out, but at specific points in the vineyard, without considering the within-field spatial variability. Therefore, considering the spatial differences within the vineyard related to the physical environment and plant growth can lead to more efficient use of phytosanitary products and better site-specific management.

Hence, two novel points have been achieved with the proposed approach and are key contributions to help in *Botrytis cinerea* control. The first is the proposal of a methodology to assess the spatial variability and the probability of *Botrytis* development in a vineyard, which takes advantage of imaging technologies, providing detailed information for each point on the field. To our knowledge, this is the first time that is considered an assessment of the BBR affection based on the study of risk maps derived from multispectral imagery, mapping the probability of *Botrytis* cinerea occurrence as a function of development factors. This method could benefit vineyard managers because detecting hot spots can be as important as knowing when the disease starts. The second key contribution is that this approach is based on risk assessment, complementary to other models, allowing a combination to optimise phytosanitary treatments by identifying the right time and place.

Finally, as noted in the present work, all the variables studied (vigour, height of the canopy, topography and canopy architecture) followed the expected behaviour, showing consistent values according to the classification group, that is, infected or healthy plants. Therefore, since the algorithm is based on biophysical variables that affect the development of the disease, there is a strong chance that this result will be observed in the majority of vineyards.

In future works, vineyards with different slopes should be studied to assess the effect of different slopes and altitudes since it is a determining variable for the explanation of the spatial variability of the disease. Another potential step forward could be the mentioned combination with the previously cited models to improve the prediction of *Botrytis*. In other words, one of the main strengths of the proposed methodology is that it could be complementary to other models (González-Domínguez et al., 2015; Hill et al., 2019; Fedele et al., 2020), i.e. including them as a prerequisite for disease development before the spatial analysis. Therefore, it will be possible to create prescription maps derived from sensors and imagery to control the disease effectively. This point should be included in any systems modelling approach for managing BBR, aiming for higher operational efficiency and reducing phytosanitary treatments, as well as economic costs. The present work presents a methodology toward accomplishing this goal that could be transferable to other woody crops, with a particular interest in evaluating other fungal diseases, as some depend on similar variables. In particular, the diseases produced by *Uncinula necator* and *Plasmopara viticola*, other fungi of great interest in viticulture. Further studies can also extend the algorithm by combining it with weather information or by including several flight missions throughout the year to capture imagery over several periods, thereby taking advantage of the benefits of time series analysis.

5. Conclusions

The presented *Botrytis* risk algorithm generates probability maps that may support vineyard managers in understanding the spatial variability of the disease. Thus, it enables the spatial 2D visualisation of the risk of BBR disease development, using UAV imagery as input. It combines photogrammetric and spatial analysis techniques, machine learning classification methods, and deep vineyard-related agronomic knowledge.

Several variables were selected as inputs to develop an algorithm that produces a heatmap using KDE to measure the risk of *Botrytis* development in vineyards. The variables employed as inputs were DTM, NDVI, CHM and LAI, estimated from the UAV images. They represent the height and architecture of the canopy, the topography and the plant status. Healthy vines were significantly different from vines affected by

Botrytis ($p < 0.05$) in each of these variables, supporting the consistency of using these inputs for the model. Furthermore, the generated heatmap could explain the risk of *Botrytis* development in the vineyard with acceptable accuracy ($R^2 > 0.7$), based on studying the spatial variability of the considered variables.

One key benefit of the presented methodology is that it takes advantage of imaging technologies that provide information about any location in the field, not only about specific points in the vineyard, such as the information given by humidity or temperature sensors. It is a promising tool demonstrating that UAV imagery alone can measure the within-field variability of *Botrytis* risk development using multispectral imagery. Furthermore, it is a first step that highlights the importance of bearing in mind the risk linked to the spatial variability of the vineyard (where and how the disease develops) and not only the risk of disease onset (when the disease starts), which other models have already considered.

Further studies may include flights at earlier phenological stages to create early *Botrytis* risk maps, or they could consist of several flights throughout the year to assess the seasonal evolution of the heatmap. Moreover, additional variables monitored from other sources, such as ground sensors, could be included in the model to improve the accuracy. However, these variables must be of agronomic significance, or they could lead to noisier maps.

CRediT authorship contribution statement

Conceptualization, **Sergio Vélez, Mar Ariza, João Valente**, Methodology, **Sergio Vélez, Mar Ariza, João Valente**, Software, **Sergio Vélez, Mar Ariza, João Valente**, Validation, **Sergio Vélez, Mar Ariza, João Valente**, Formal analysis, **Sergio Vélez, Mar Ariza, João Valente**, Investigation, **Sergio Vélez, Mar Ariza, João Valente**, Resources, **Sergio Vélez, Mar Ariza, João Valente**, Data curation, **Sergio Vélez, Mar Ariza, João Valente**, Writing – original draft, **Sergio Vélez, Mar Ariza**, Writing – review & editing, **João Valente**, Visualization, **Sergio Vélez, Mar Ariza, João Valente**, Supervision, **Sergio Vélez, João Valente**, Project administration, **João Valente**, Funding acquisition, **João Valente**.

Declaration of Competing Interest

The authors declare that they have no known competing financial interests or personal relationships that could have appeared to influence the work reported in this paper.

Data availability

Data is available here: 10.5281/zenodo.7064895.

Acknowledgements

References

Agrios, G.N., 2005. Plant Pathology, fifth ed. Elsevier Academic Press.

Anon, 2001. Botryotinia fuckeliana on grapevine. EPPO Bull. 31 (2), 299–302. doi: 10.1111/j.1365-2338.2001.tb00997.x.

Ammoniaci, M., Kartsiotis, S.-P., Perria, R., Storchi, P., 2021. State of the art of monitoring technologies and data processing for precision viticulture. Agriculture 11 (3), 201. https://doi.org/10.3390/agriculture11030201.

Anastasiou, E., Balafoutis, A., Darra, N., Psiroukis, V., Biniari, A., Xanthopoulos, G., Fountas, S., 2018. Satellite and proximal sensing to estimate the yield and quality of table grapes. Agriculture 8 (7), 94. https://doi.org/10.3390/agriculture8070094.

Avtar, R., Watanabe, T., 2020. Unmanned Aerial Vehicle: Applications in Agriculture and Environment. Springer International Publishing. https://doi.org/10.1007/978-3-030-27157-2.

Baddeley, A., Rubak, E., Turner, R., 2016. Spatial Point Patterns.

Baeza, P., Sánchez-De-Miguel, P., Lissarrague, J.R., 2010. Radiation balance in vineyards. In: Delrot, S., Medrano, H., Or, E., Bavaresco, L., Grando, S. (Eds.), Methodologies and Results in Grapevine Research. Springer, Netherlands, pp. 21–29. https://doi.org/10.1007/978-90-481-9283-0_2.

Baluja, J., Diago, M.P., Balda, P., Zorer, R., Meggio, F., Morales, F., Tardaguila, J., 2012. Assessment of vineyard water status variability by thermal and multispectral imagery using an unmanned aerial vehicle (UAV). Irrig. Sci. 30 (6), 511–522. https://doi.org/10.1007/s00271-012-0382-9.

Bois, B., Zito, S., Calonnec, A., 2017. Climate vs grapevine pests and diseases worldwide: the first results of a global survey. OENO One 51 (2), 133. https://doi.org/10.20870/oeno-one.2016.0.0.1780.

Burchett, S., Burchett, S., 2017. Plant Pathology. Garland Science, Taylor & Francis Group.

Campos, J., García-Ruíz, F., Gil, E., 2021. Assessment of vineyard canopy characteristics from vigour maps obtained using UAV and Satellite imagery. Sensors 21 (7), 2363. https://doi.org/10.3390/s21072363.

Campos, J., Llop, J., Gallart, M., García-Ruiz, F., Gras, A., Salcedo, R., Gil, E., 2019. Development of canopy vigour maps using UAV for site-specific management during vineyard spraying process. Precis. Agric. 20 (6), 1136–1156. https://doi.org/10.1007/s11119-019-09643-z.

Cancela, J.J., Fandiño, M., Rey, B.J., Dafonte, J., González, X.P., 2017. Discrimination of irrigation water management effects in pergola trellis system vineyards using a vegetation and soil index. Agric. Water Manag. 183, 70–77. https://doi.org/10.1016/j.agwat.2016.11.003.

Carrivick, J. L., Smith, M. W., Quincey, D. J., 2016. Structure from Motion in the Geosciences. doi: 10.1002/9781118895818.

Cotoras, M., García, C., Mendoza, L., 2009. *Botrytis cinerea* isolates collected from grapes present different requirements for conidia germination. Mycologia 101 (3), 287–295. https://doi.org/10.3852/08-012.

Creasy, G.L., Creasy, L.L., 2009. Grapes. CABI.

Daglio, G., Cesaro, P., Todeschini, V., Lingua, G., Lazzari, M., Berta, G., Massa, N., 2022. Potential field detection of Flavescence dorée and Esca diseases using a ground sensing optical system. Biosyst. Eng. 215, 203–214. https://doi.org/10.1016/j.biosystemseng.2022.01.009.

Damialis, A., Kaimakamis, E., Konoglou, M., Akritidis, I., Traidl-Hoffmann, C., Gioulekas, D., 2017. Estimating the abundance of airborne pollen and fungal spores at variable elevations using an aircraft: how high can they fly? Sci. Rep. 7 (1), 44535. https://doi.org/10.1038/srep44535.

del-Campo-Sanchez, A., Ballesteros, R., Hernandez-Lopez, D., Ortega, J.F., Moreno, M.A., on behalf of Agroforestry and Cartography Precision Research Group, 2019. Quantifying the effect of Jacobiasca lybica pest on vineyards with UAVs by combining geometric and computer vision techniques. PLoS One 14 (4), e0215521. https://doi.org/10.1371/journal.pone.0215521.

Deytieux-Belleau, C., Geny, L., Roudet, J., Mayet, V., Donèche, B., Fermaud, M., 2009. Grape berry skin features related to ontogenic resistance to Botrytis cinerea. Eur. J. Plant Pathol. 125 (4), 551–563. https://doi.org/10.1007/s10658-009-9503-6.

Diggle, P.J., 2013. Statistical Analysis of Spatial and Spatio-Temporal Point Patterns, 0 ed. Chapman and Hall/CRC. https://doi.org/10.1201/b15326.

Elad, Y., Williamson, B., Tudzynski, P., Delen, N., Elad, Y., 2007. Botrytis: Biology, Pathology and Control. Springer.

Elmer, P.A.G., Michailides, T.J., 2007. Epidemiology of Botrytis cinerea in Orchard and Vine Crops. In: Elad, Y., Williamson, B., Tudzynski, P., Delen, N. (Eds.), Botrytis: Biology, Pathology and Control. Springer, Netherlands, pp. 243–272. https://doi.org/10.1007/978-1-4020-2626-3_14.

Fedele, G., González-Domínguez, E., Delière, L., Díez-Navajas, A.M., Rossi, V., 2020. Consideration of latent infections improves the prediction of Botrytis bunch rot severity in vineyards. Plant Dis. 104 (5), 1291–1297. https://doi.org/10.1094/PDIS-11-19-2309-RE.

Ferrer, M., Echeverría, G., Pereyra, G., Gonzalez-Neves, G., Pan, D., Mirás-Avalos, J.M., 2020. Mapping vineyard vigor using airborne remote sensing: relations with yield, berry composition and sanitary status under humid climate conditions. Precis. Agric. 21 (1), 178–197. https://doi.org/10.1007/s11119-019-09663-9.

Font, D., Tresanchez, M., Martínez, D., Moreno, J., Clotet, E., Palacín, J., 2015. Vineyard yield estimation based on the analysis of high resolution images obtained with artificial illumination at night. Sensors 15 (4), 8284–8301. https://doi.org/10.3390/s150408284.

Fuentes, S., Poblete-Echeverría, C., Ortega-Farias, S., Tyerman, S., De Bei, R., 2014. Automated estimation of leaf area index from grapevine canopies using cover photography, video and computational analysis methods: New automated canopy vigour monitoring tool. Aust. J. Grape Wine Res. 20 (3), 465–473. https://doi.org/10.1111/ajgw.12098.

Gatti, M., Garavani, A., Vercesi, A., Poni, S., 2017. Ground-truthing of remotely sensed within-field variability in a cv. Barbera plot for improving vineyard management: vigour mapping and vineyard management. Aust. J. Grape Wine Res. 23 (3), 399–408. https://doi.org/10.1111/ajgw.12286.

Geetha, V., Punitha, A., Abarna, M., Akshaya, M., Illakiya, S., Janani, A. P., 2020. An effective crop prediction using random forest algorithm. In: Proceedings of the International Conference on System, Computation, Automation and Networking (ICSCAN), 2020 , 1–5. doi: 10.1109/ICSCAN49426.2020.9262311.

Giovos, R., Tassopoulos, D., Kalivas, D., Lougkos, N., Priovolou, A., 2021. Remote sensing vegetation indices in viticulture: a critical review. Agriculture 11 (5), 457. https://doi.org/10.3390/agriculture11050457.

Gongal, A., Amatya, S., Karkee, M., Zhang, Q., Lewis, K., 2015. Sensors and systems for fruit detection and localization: a review. Comput. Electron. Agric. 116, 8–19. https://doi.org/10.1016/j.compag.2015.05.021.

González-Domínguez, E., Caffi, T., Ciliberti, N., Rossi, V., 2015. A mechanistic model of botrytis cinerea on grapevines that includes weather, vine growth stage, and the main infection pathways. PLoS One 10 (10), e0140444. https://doi.org/10.1371/journal.pone.0140444.

González-Domínguez, E., Fedele, G., Caffi, T., Delière, L., Sauris, P., Gramaje, D., Ramos-Saez de Ojer, J.L., Díaz-Losada, E., Díez-Navajas, A.M., Bengoa, P., Rossi, V., 2019. A network meta-analysis provides new insight into fungicide scheduling for the control of Botrytis cinerea in vineyards: meta-analysis Botrytis bunch rot control. Pest Manag. Sci. 75 (2), 324–332. https://doi.org/10.1002/ps.5116.

Hidalgo, J., 2006. La calidad del vino desde el viñedo. Mundi-Prensa https://library.biblioboard.com/content/b3757450-cf67-43ec-a66a-42dc96227c98.

Hill, G.N., Beresford, R.M., Evans, K.J., 2019. Automated analysis of aggregated datasets to identify climatic predictors of botrytis bunch rot in wine grapes. Phytopathology® 109 (1), 84–95. https://doi.org/10.1094/PHYTO-10-17-0357-R.

Horne, J.S., Garton, E.O., 2006. Likelihood cross-validation versus least squares cross-validation for choosing the smoothing parameter in kernel home-range analysis. J. Wildl. Manag. 70 (3), 641–648. https://doi.org/10.2193/0022-541X(2006)70[641:LCVLSC]2.0.CO;2.

Johnson, L.F., Bosch, D.F., Williams, D.C., Lobitz, B.M., 2001. Remote sensing of vineyard management zones: implications for wine quality. Appl. Eng. Agric. 17 (4) https://doi.org/10.13031/2013.6454.

Johnson, L.F., Roczen, D.E., Youkhana, S.K., Nemani, R.R., Bosch, D.F., 2003. Mapping vineyard leaf area with multispectral satellite imagery. Comput. Electron. Agric. 38 (1), 33–44. https://doi.org/10.1016/S0168-1699(02)00106-0.

Keller, M., 2015. The Science of Grapevines: Anatomy and Physiology, second ed. Academic Press is an imprint of Elsevier.

Keller, M., Kummer, M., Vasconcelos, M.C., 2001. Reproductive growth of grapevines in response to nitrogen supply and rootstock. Aust. J. Grape Wine Res. 7 (1), 12–18. https://doi.org/10.1111/j.1755-0238.2001.tb00188.x.

Keller, M., Viret, O., Cole, F.M., 2003. Botrytis cinerea Infection in grape flowers: defense reaction, latency, and disease expression. Phytopathology 93 (3), 316–322. https://doi.org/10.1094/PHYTO.2003.93.3.316.

Kosuge, T., Hewitt, W.B., 1964. Exudate of grape berries and their effect on germination of conidia of Botrytis cinerea. Phytopathology 54, 167–172.

Kraus, C., Pennington, T., Herzog, K., Hecht, A., Fischer, M., Voegele, R.T., Hoffmann, C., Töpfer, R., Kicherer, A., 2018. Effects of canopy architecture and microclimate on grapevine health in two training systems. Vitis J. Grapevine Res. 53–60. https://doi.org/10.5073/VITIS.2018.57.53-60.

Kretschmer, M., Kassemeyer, H.-H., Hahn, M., 2007. Age-dependent Grey Mould Susceptibility and Tissue-specific Defence Gene Activation of Grapevine Berry Skins after Infection by Botrytis cinerea. J. Phytopathol. 155 (5), 258–263. https://doi.org/10.1111/j.1439-0434.2007.01216.x.

Ledderhof, D., Brown, R., Reynolds, A., Jollineau, M., 2016. Using Remote Sensing to Understand Pinot noir Vineyard Variability in Ontario. 96, 20.

Loggenberg, K., Strever, A., Greyling, B., Poona, N., 2018. Modelling water stress in a shiraz vineyard using hyperspectral imaging and machine learning. Remote Sens. 10 (2), 202. https://doi.org/10.3390/rs10020202.

Lopez Pinar, A., Rauhut, D., Ruehl, E., Buettner, A., 2017. Effects of bunch rot (Botrytis cinerea) and powdery mildew (Erysiphe necator) fungal diseases on wine aroma. Front. Chem. 5. https://doi.org/10.3389/fchem.2017.00020.

Marciniak, M., Brown, R., Reynolds, A., Jollineau, M., 2015. Use of remote sensing to understand the terroir of the Niagara Peninsula. Applications in a Riesling vineyard. OENO One 49 (1), 1. https://doi.org/10.20870/oeno-one.2015.49.1.97.

Matese, A., Di Gennaro, S.F., 2021. Beyond the traditional NDVI index as a key factor to mainstream the use of UAV in precision viticulture. Sci. Rep. 11 (1), 2721. https://doi.org/10.1038/s41598-021-81652-3.

Messina, G., Praticò, S., Badagliacca, G., Di Fazio, S., Monti, M., Modica, G., 2021. Monitoring onion crop "Cipolla Rossa di Tropea Calabria IGP" growth and yield response to varying nitrogen fertilizer application rates using UAV imagery. Drones 5 (3), 61. https://doi.org/10.3390/drones5030061.

Molitor, D., Baus, O., Hoffmann, L., Beyer, M., 2016. Meteorological conditions determine the thermal-temporal position of the annual Botrytis bunch rot epidemic on Vitis vinifera L. cv. Riesling grapes. OENO One 50 (3). https://doi.org/10.20870/oeno-one.2016.50.3.36.

Pádua, L., Marques, P., Adão, T., Guimarães, N., Sousa, A., Peres, E., Sousa, J.J., 2019. Vineyard variability analysis through UAV-based vigour maps to assess climate change impacts. Agronomy 9 (10), 581. https://doi.org/10.3390/agronomy9100581.

Pañitrur-De la Fuente, C., Valdés-Gómez, H., Roudet, J., Verdugo-Vásquez, N., Mirabal, Y., Laurie, V.F., Goutouly, J.P., Acevedo Opazo, C., Fermaud, M., 2020. Vigor thresholded NDVI is a key early risk indicator of Botrytis bunch rot in vineyards. OENO One 54 (2), 279–297. https://doi.org/10.20870/oeno-one.2020.54.2.2954.

Radoglou-Grammatikis, P., Sarigiannidis, P., Lagkas, T., Moscholios, I., 2020. A compilation of UAV applications for precision agriculture. Comput. Netw. 172, 107148 https://doi.org/10.1016/j.comnet.2020.107148.

Reich, J., Chatterton, S., Johnson, D., 2017. Temporal Dynamics of Botrytis cinerea and Sclerotinia sclerotiorum in Seed Alfalfa Fields of Southern Alberta, Canada. Plant Dis. 101 (2), 331–343. https://doi.org/10.1094/PDIS-04-16-0492-RE.

Rodríguez-Rajo, F.J., Jato, V., Fernández-González, M., Aira, M.J., 2010. The use of aerobiological methods for forecasting Botrytis spore concentrations in a vineyard. Grana 49 (1), 56–65. https://doi.org/10.1080/00173130903472393.

Rouse, W., Haas, R.H., Welland J.A., Deering D.W., 1973. Monitoring vegetation systems in the great plains with ERTS. In: Proceedings of the Third ERTS Symposium, NASA, 10–14, 309–317.

Siebring, J., Valente, J., Domingues Franceschini, M.H., Kamp, J., Kooistra, L., 2019. Object-Based image analysis applied to low altitude aerial imagery for potato plant trait retrieval and pathogen detection. Sensors 19 (24), 5477. https://doi.org/10.3390/s19245477.

Silverman, B.W., 2018. Density Estimation for Statistics and Data Analysis, first ed. Routledge. https://doi.org/10.1201/9781315140919.

Smart, R.E., Dick, J.K., Gravett, I.M., Fisher, B.M., 2017. Canopy management to improve grape yield and wine quality—principles and practices. South Afr. J. Enol. Vitic. 11 (1) https://doi.org/10.21548/11-1-2232.

Snyder, R.L., Abreu, J.P. de M.-, 2005. Frost Protection: Fundamentals, Practice, and Economics, 1. Richard L. Snyder; J. Paulo de Melo-Abreu.

Sun, L., Gao, F., Anderson, M., Kustas, W., Alsina, M., Sanchez, L., Sams, B., McKee, L., Dulaney, W., White, W., Alfieri, J., Prueger, J., Melton, F., Post, K., 2017. Daily mapping of 30 m LAI and NDVI for grape yield prediction in California vineyards. Remote Sens. 9 (4), 317. https://doi.org/10.3390/rs9040317.

Tello, J., Ibáñez, J., 2018. What do we know about grapevine bunch compactness? A state-of-the-art review: review on bunch compactness. Aust. J. Grape Wine Res. 24 (1), 6–23. https://doi.org/10.1111/ajgw.12310.

Torres-Sánchez, J., Mesas-Carrascosa, F.J., Santesteban, L.-G., Jiménez-Brenes, F.M., Oneka, O., Villa-Llop, A., Loidi, M., López-Granados, F., 2021. Grape cluster detection using UAV photogrammetric point clouds as a low-cost tool for yield forecasting in vineyards. Sensors 21 (9), 3083. https://doi.org/10.3390/s21093083.

Towers, P.C., Strever, A., Poblete-Echeverría, C., 2019. Comparison of vegetation indices for leaf area index estimation in vertical shoot positioned vine canopies with and without grenbiule hail-protection netting. Remote Sens. 11 (9), 1073. https://doi.org/10.3390/rs11091073.

Urretavizcaya, I., Santesteban, L.G., Tisseyre, B., Guillaume, S., Miranda, C., Royo, J.B., 2014. Oenological significance of vineyard management zones delineated using early grape sampling. Precis. Agric. 15 (1), 111–129. https://doi.org/10.1007/s11119-013-9328-3.

Valdés-Gómez, H., Fermaud, M., Roudet, J., Calonnec, A., Gary, C., 2008. Grey mould incidence is reduced on grapevines with lower vegetative and reproductive growth. Crop Prot. 27 (8), 1174–1186. https://doi.org/10.1016/j.cropro.2008.02.003.

Vélez, S., Ariza-Sentís, M., Valente, J., 2022. UAV multispectral imagery dataset over a vineyard affected by Botrytis in "Tomiño", Pontevedra, Spain. Includes GPS location of diseases and GCP points. (Data set), Zenodo. doi: 10.5281/zenodo.7064895.

Vélez, S., Barajas, E., Rubio, J.A., Vacas, R., Poblete-Echeverría, C., 2020. Effect of missing vines on total leaf area determined by ndvi calculated from sentinel satellite data: progressive vine removal experiments. Appl. Sci. 10 (10), 3612. https://doi.org/10.3390/app10103612.

Vélez, S., Poblete-Echeverría, C., Rubio, J.A., Vacas, R., Barajas, E., 2021. Estimation of Leaf Area Index in vineyards by analysing projected shadows using UAV imagery. OENO One 55 (4), 159–180. https://doi.org/10.20870/oeno-one.2021.55.4.4639.

White, R.E., 2015. Understanding Vineyard Soils, second ed. Oxford University Press.

Williamson, B., Duncan, G.H., Harrison, J.G., Harding, L.A., Elad, Y., Zimand, G., 1995. Effect of humidity on infection of rose petals by dry-inoculated conidia of Botrytis cinerea. Mycol. Res. 99 (11), 1303–1310. https://doi.org/10.1016/S0953-7562(09)81212-4.

Würz, D. A., Brighenti, A. F., Souza, D. S., Reinher, J., Canossa, A., Rufato, L., 2021. Early leaf removal as strategy to reduce botrytis bunch rot on chardonnay grapevine in high altitude region of Santa Catarina State, 20(3), 7.

Würz, D.A., Rufato, L., Bogo, A., Allebrandt, R., Pereira de Bem, B., Marcon Filho, J.L., Brighenti, A.F., Bonin, B.F., 2020. Effects of leaf removal on grape cluster architecture and control of Botrytis bunch rot in Sauvignon Blanc grapevines in Southern Brazil. Crop Prot. 131, 105079 https://doi.org/10.1016/j.cropro.2020.105079.

Xie, T., Li, J., Yang, C., Jiang, Z., Chen, Y., Guo, L., Zhang, J., 2021. Crop height estimation based on UAV images: methods, errors, and strategies. Comput. Electron. Agric. 185, 106155 https://doi.org/10.1016/j.compag.2021.106155.

Yang, C., 2020. Remote sensing and precision agriculture technologies for crop disease detection and management with a practical application example. Engineering 6 (5), 528–532. https://doi.org/10.1016/j.eng.2019.10.015.

Zhang, C., Valente, J., Kooistra, L., Guo, L., Wang, W., 2021. Orchard management with small unmanned aerial vehicles: a survey of sensing and analysis approaches. Precis. Agric. 22 (6), 2007–2052. https://doi.org/10.1007/s11119-021-09813-y.